Title

A Pan1/End3/Sla1 complex links Arp2/3-mediated actin assembly to sites of clathrin-mediated endocytosis

Journal

Molecular Biology of the Cell, 26(21)

ISSN

1059-1524

Authors

Sun, Yidi
Leong, Nicole T
Wong, Tiffany
et al.

Publication Date

2015-11-01

DOI

10.1091/mbc.e15-04-0252

Peer reviewed

A Pan1/End3/Sla1 complex links Arp2/3-mediated actin assembly to sites of clathrin-mediated endocytosis

Yidi Sun, Nicole T. Leong, Tiffany Wong, and David G. Drubin
Department of Molecular and Cell Biology, University of California, Berkeley, Berkeley, CA 94720

ABSTRACT **More than 60 highly conserved proteins appear sequentially at sites of clathrin-mediated endocytosis in yeast and mammals. The yeast Eps15-related proteins Pan1 and End3 and the CIN85-related protein Sla1 are known to interact with each other in vitro, and they all appear after endocytic-site initiation but before endocytic actin assembly, which facilitates membrane invagination/scission. Here we used live-cell imaging in parallel with genetics and biochemistry to explore comprehensively the dynamic interactions and functions of Pan1, End3, and Sla1. Our results indicate that Pan1 and End3 associate in a stable manner and appear at endocytic sites before Sla1. The End3 C-terminus is necessary and sufficient for its cortical localization via interaction with Pan1, whereas the End3 N-terminus plays a crucial role in Sla1 recruitment. We systematically examined the dynamic behaviors of endocytic proteins in cells in which Pan1 and End3 were simultaneously eliminated, using the auxin-inducible degron system. The results lead us to propose that endocytic-site initiation and actin assembly are separable processes linked by a Pan1/End3/Sla1 complex. Finally, our study provides mechanistic insights into how Pan1 and End3 function with Sla1 to coordinate cargo capture with actin assembly.**

Monitoring Editor
Thomas D. Pollard
Yale University

Received: Apr 29, 2015
Revised: Aug 21, 2015
Accepted: Aug 27, 2015

INTRODUCTION

In the past decade, the precise timing of the appearance of >60 highly conserved proteins at sites of clathrin-mediated endocytosis (CME) and their detailed localization along the invaginated membrane have been revealed and found to be similar from yeast to mammals (McMahon and Boucrot, 2011; Boettner *et al.*, 2012; Figure 1, A and B). The yeast proteins have been grouped into several modules based on their dynamics, interactions, and functions: early module, early coat module, coat module, WASP/MYOSIN module, actin module, and amphiphysin module (Weinberg and Drubin, 2012; Figure 1A).

From a temporal perspective, yeast endocytosis can be divided into an early phase and a late phase (Carroll *et al.*, 2012; Brach *et al.*, 2014; Figure 1A). The proteins that arrive during the early phase (including mostly early module and early coat module proteins) generally exhibit longer and more variable lifetimes than proteins that arrive during the late phase (including coat module, WASP/MYOSIN module, actin module, and amphiphysin module proteins), which exhibit shorter and more regular lifetimes (Weinberg and Drubin, 2012). The early-phase proteins likely function in determining endocytic-site location and recruiting cargo (Brach *et al.*, 2014). Key functions of the late-phase proteins are to induce deeply invaginated membranes and facilitate scission, in part by inducing actin assembly (Mooren *et al.*, 2012), which occurs in a burst late in the CME pathway in both yeast (Kaksonen *et al.*, 2003) and mammalian cells (Merrifield *et al.*, 2002).

In vitro reconstitution studies demonstrated that the late-phase protein Las17 (yeast Wiskott–Aldrich syndrome protein [WASP]) is sufficient to assemble endocytic actin networks around microbeads in yeast cell extracts (Michelot *et al.*, 2010). Of interest, these actin networks contain most late-phase endocytic proteins but mostly lack the early-phase and coat module proteins (Michelot *et al.*, 2010). The observation that endocytic vesicle formation can still occur even when genes encoding several early-phase proteins are simultaneously deleted suggests a degree of autonomy in the execution of steps in the pathway (Brach *et al.*, 2014). These studies

This article was published online ahead of print in MBoC in Press (http://www.molbiolcell.org/cgi/doi/10.1091/mbc.E15-04-0252) on September 2, 2015.

Address correspondence to: David G. Drubin (drubin@berkeley.edu).

Abbreviations used: a.a, amino acid; AID, auxin-inducible degron; CME, clathrin-mediated endocytosis; MIP, maximum intensity projections; WASP, Wiskott–Aldrich syndrome protein.

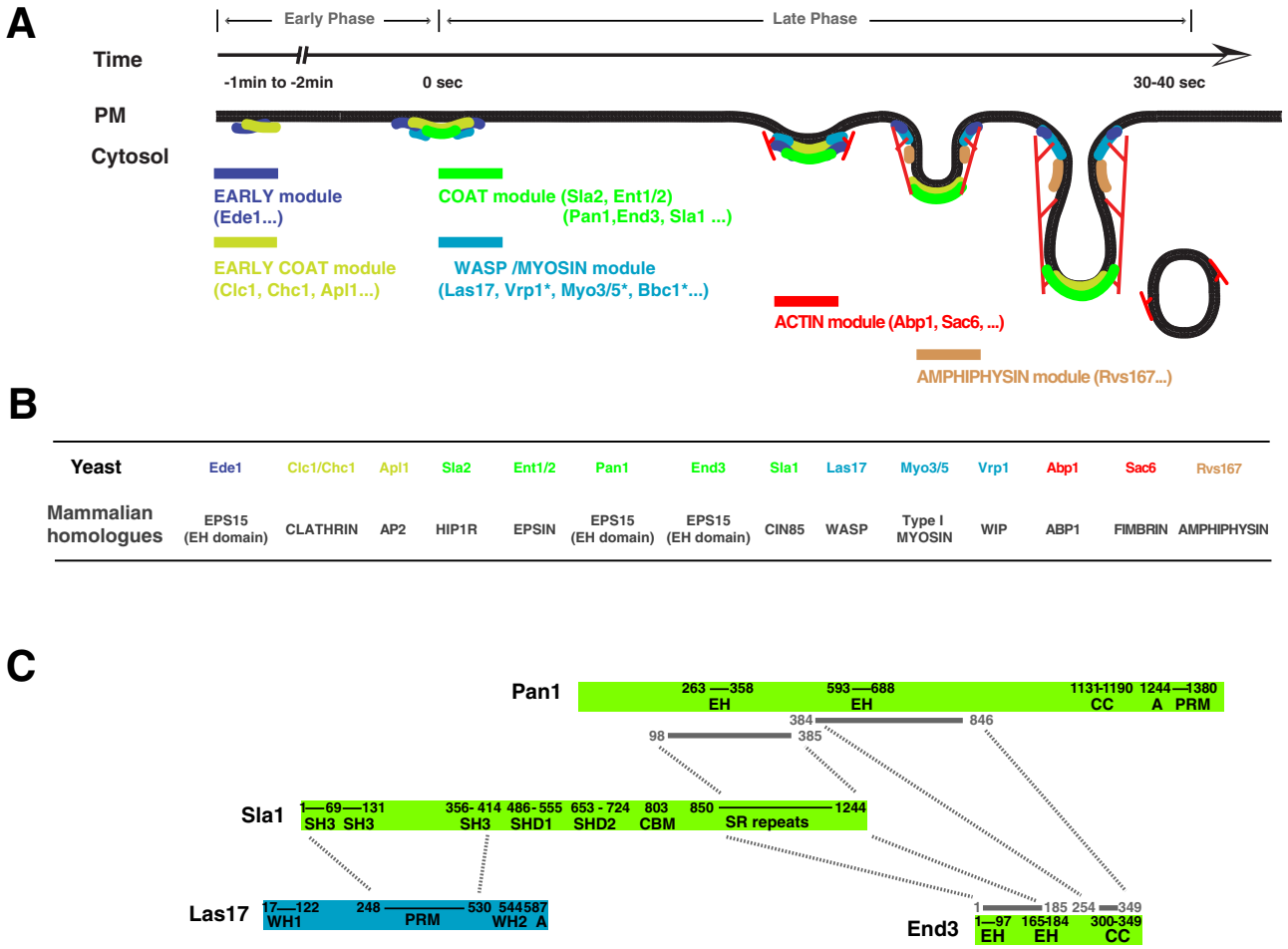

FIGURE 1: Endocytic internalization timeline and interactions between Pan1, End3, Sla1, and Las17 in vitro. (A) Spatial-temporal recruitment of endocytic proteins. Endocytic proteins may be grouped into six modules, with defining proteins in parentheses. Note that proteins of the WASP/MYOSIN module arrive at endocytic sites with different timing. Las17 arrives with similar timing to coat module proteins, and Vrp1, Myo5, and Bbc1 arrive later (Sun *et al.*, 2006). (B) Key yeast endocytic proteins and their mammalian homologues. (C) Previously reported in vitro interactions between Pan1, End3, Sla1, and Las17. Each pair of the dotted lines connects the regions through which two indicated proteins interact physically in vitro (Tang *et al.*, 2000; Rodal *et al.*, 2003; Feliciano and Di Pietro, 2012). A, acidic; CBM, clathrin box motif; CC, coiled-coil domain; EH, Eps15 homology; PRM, proline-rich domain; SH3, Src homology 3; SHD1, Sla1 homology domain 1; SHD2, Sla1 homology domain 2; SR repeats, LxxQxTG repeats; WH1, WASP homology 1; WH2, WASP homology 2.

raise several fundamental questions for understanding how endocytic sites form and mature. Do endocytic-site formation and maturation consist of functionally independent phases, such as an initiation phase and an actin assembly phase, or are they interdependent? If the phases are independent, how are they linked to each other? In particular, how is the early event of cargo capture coordinated with the late event of actin assembly?

To address these questions, this study focuses on proteins recruited at the transition between the early coat assembly and cargo capture phases and late actin assembly phases. These proteins are candidates for coupling actin assembly to early endocytic events. Two crucial groups of highly conserved coat module proteins arrive at the junction between the early and late phases: Sla2/Ent1/2 (yeast HIP1R and yeast epsin) and Pan1/End3/Sla1 (yeast Eps15 and yeast CIN85). Sla2 and Ent1/2 function as essential molecular linkers that transmit forces generated by the actin cytoskeleton to the plasma membrane (Kaksonen *et al.*, 2003; Sun *et al.*, 2005; Skruzny *et al.*, 2012). Pan1, End3, and Sla1 play roles in endocytosis and cell growth, which range from crucial (Pan1 and End3) to less important (Sla1; Sachs and Deardorff, 1992; Benedetti *et al.*, 1994; Wendland *et al.*, 1996). In vitro studies suggested that Pan1, End3, and Sla1 interact with each other in a heterotrimeric complex (Tang *et al.*, 2000; Figure 1C). However, how and when these three proteins interact in vivo and how such interactions relate to the endocytic function are not clear. This lack of information is mainly due to the fact that most of the previous studies focused on the functions of individual proteins or particular domains (Duncan *et al.*, 2001; Confalonieri and Di Fiore, 2002; Howard *et al.*, 2002; Rodal *et al.*, 2003; Feliciano and Di Pietro, 2012; Suzuki *et al.*, 2012; Whitworth *et al.*, 2014). Of interest, Sla1 was previously identified as a cargo adaptor (Howard *et al.*, 2002), and a recent study suggested that Pan1 plays a role in regulating transitions between endocytic stages (Bradford *et al.*, 2015). Thus careful investigation of Pan1-End3-Sla1 interactions and functions in vivo promises to answer the fundamental questions posed earlier.

Here we used live-cell imaging in parallel with genetics and biochemistry to investigate how Pan1, End3, and Sla1 cooperate during CME. Our studies revealed a molecular basis for coordination between receptors, adaptors, and actin assembly at endocytic sites.

RESULTS

Pan1 and End3 associate in a stable manner and appear at endocytic sites before Sla1 and Las17

Previous studies revealed that the endocytic coat proteins Pan1, End3, and Sla1 interact with each other physically in vitro (Tang *et al.*, 2000; Figure 1C). Subsequent live-cell imaging studies suggested that these three proteins are recruited to endocytic sites with roughly similar timing (around 30 s before vesicle scission; Kaksonen *et al.*, 2003, 2005; Feliciano and Di Pietro, 2012). However, a study analyzing proteins in yeast cell extracts suggested that Sla1 is associated with Las17 in a large, stable complex lacking End3 (Feliciano and Di Pietro, 2012). To investigate spatial-temporal relationships between Pan1, End3, Sla1, and Las17 in vivo, we performed two-color live-cell imaging on these proteins. The data were analyzed and quantified using open-source Icy image analysis software (de Chaumont *et al.*, 2012; see *Materials and Methods*). Pan1-GFP appears at the cell cortex ~6 s before Sla1-mCherry (Figure 2A and Supplemental Movie S1). Similar results were obtained when Pan1 was fused to mCherry and Sla1 was fused to green fluorescent protein (GFP; Figure 2A and Supplemental Movie S1), indicating that the difference in appearance time of Pan1 and Sla1 at the cell cortex was not due to the fluorescence properties of GFP and mCherry. Consistently, Sla1-GFP patches reach 50% of the maximum fluorescence intensity ~8 s after Pan1-mCherry patches (Figure 2B; *Materials and Methods*). In contrast, Pan1-mCherry and End3-GFP were recruited to the cell cortex with indistinguishable kinetic profiles (Figure 2, A and C, and Supplemental Movie S2), as were Sla1-mCherry and Las17-GFP (Feliciano and Di Pietro, 2012; Figure 2A and Supplemental Movie S2). Las17-GFP appeared after Pan1-mCherry in a manner similar to Sla1 (Figure 2A and Supplemental Movie S1). These results demonstrate that Pan1 and End3 arrive at endocytic sites simultaneously and before Sla1 and Las17. On the other hand, consistent with previous findings (Weinberg and Drubin, 2012), Pan1, End3, and Sla1 move into the cytoplasm at the end of their lifetimes, whereas Las17 does not (Figure 2A). The inward patch movement is believed to correspond to movement with the invaginating endocytic membrane and nascent vesicle (Kaksonen *et al.*, 2003). Thus these results suggest that Pan1, End3, and Sla1 localize to the budding vesicle, whereas Las17 localizes at the base and possibly the tubule of the invaginated membrane. Together these results demonstrate that Pan1 shares indistinguishable spatiotemporal behavior with End3 but not with Sla1 or Las17. Moreover, Sla1 and Las17 appear at endocytic sites with similar timing but separate from each other at the endocytic membrane invagination step, indicating that Sla1 and Las17 do not associate with each other continuously in vivo.

To gain additional insight into how Pan1, End3, Sla1, and Las17 interact with each other, we performed gel filtration analysis of yeast cell extracts. We previously established a method to prepare yeast cell extracts that are competent to reconstitute endocytic actin network assembly on Las17-coated microbeads (Michelot *et al.*, 2010). Such yeast cell extracts were separated by size-exclusion chromatography, and the resulting fractions were analyzed by immunoblotting. As shown in Figure 3, A and B, Pan1 and End3 show nearly identical elution profiles. Immunoprecipitation analysis further confirmed that End3 and Pan1 are physically associated in the same complexes (Figure 3C). On the other hand, the gel filtration analysis revealed that the majority of Las17 did not elute in the same fractions as End3 and Pan1 (Figure 3, A and B). Furthermore, although Sla1 cofractionated with both Pan1 and End3, it has a broader fractionation range and was also present in Las17-containing fractions. Together these results support the conclusions that Pan1 associates with End3 in a stable manner and that Pan1 and End3 are not always present in the same protein complexes with Sla1 and Las17.

The End3 C-terminus is necessary and sufficient for End3 cortical localization via interaction with Pan1

As shown in the foregoing section, Pan1 and End3 share similar dynamic behavior during endocytic internalization and appear to exist the same protein complex. We next examined the functional interrelationship between these two proteins.

Because Pan1 is essential for cell growth, exploring its function by making a null allele has not been possible. We therefore used the recently developed auxin-inducible degron system (Nishimura *et al.*, 2009; Eng *et al.*, 2014) for the rapid depletion of auxin-inducible degron (AID)–tagged Pan1 in live cells and examined the dynamic behavior of End3 in these cells. Control experiments indicate that 250 µM auxin is not toxic for our strain background and is sufficient to rapidly deplete Pan1 (Supplemental Figure S1). In the absence of auxin, the *PAN1-AID TIR1* strain expresses Pan1 at normal levels (Supplemental Figure S1B), and End3-GFP patches form at the cell cortex and move inward at the end of their normal lifetime (around 30 s; Figure 4A and Supplemental Movie S3; Kaksonen *et al.*, 2005). After 60 min of treatment with 250 µM auxin, Pan1 was undetectable in the *PAN1-AID TIR1* strain (Supplemental Figure S1B). Of importance, End3-GFP cortical localization was reduced by 77% (from 1.83 ± 0.52 to 0.42 ± 0.15 patches/µm; *Materials and Methods*) when Pan1 was depleted (Figure 4A and Supplemental Movie S3), and correspondingly more End3-GFP was diffuse in the cytoplasm (Figure 4A and Supplemental Movie S3). These results establish that End3 cortical localization is highly dependent on Pan1. In contrast, Pan1 cortical recruitment is largely independent of End3 because Pan1-GFP still localizes to cortical patches in *end3Δ* cells (Figure 4B and Supplemental Movie S4). However, in *end3Δ* cells, Pan1-GFP patches stay nonmotile on the cell cortex during a 2-min movie (Figure 4B and Supplemental Movie S4), indicating that endocytic vesicle formation is impaired.

The End3 C-terminus was previously shown to bind directly to the middle of Pan1 in vitro (Tang *et al.*, 1997; Whitworth *et al.*, 2014; Figure 1C). Because Pan1 plays a key role in End3 cortical recruitment (Figure 4A), we examined whether the End3 C-terminus is required for such recruitment. As shown in Figure 4C, End3 1-254 a.a.–GFP appeared mostly in the cytoplasm, whereas End3 185-349 a.a.–GFP was localized to patches on the cell cortex, indicating that the End3 C-terminus is necessary and sufficient for its recruitment to cortical patches (Supplemental Movie S5). These results support the idea that End3 is recruited to endocytic sites through interaction of its C-terminus with Pan1. We observed that *end3 185-349 a.a.–GFP* cells are sick at 37°C, similar to *end3Δ* cells (Figures 4B and 3C and Supplemental Figure S2), which suggests that whereas the C-terminus is required for End3 localization, End3's N-terminus provides important functions.

When gel filtration analysis was performed on *end3 1-254 a.a.–GFP* cell extracts, the elution volume of End3 1-254 a.a.–GFP was dramatically shifted relative to wild-type End3-GFP (compare Figures 3A and 4D). A similar shift was also observed when gel filtration analysis was performed on cell extracts from which Pan1 was eliminated using the auxin-inducible degron system (Figure 4E). In contrast, End3 185-349 a.a.–GFP still cofractionated with Pan1

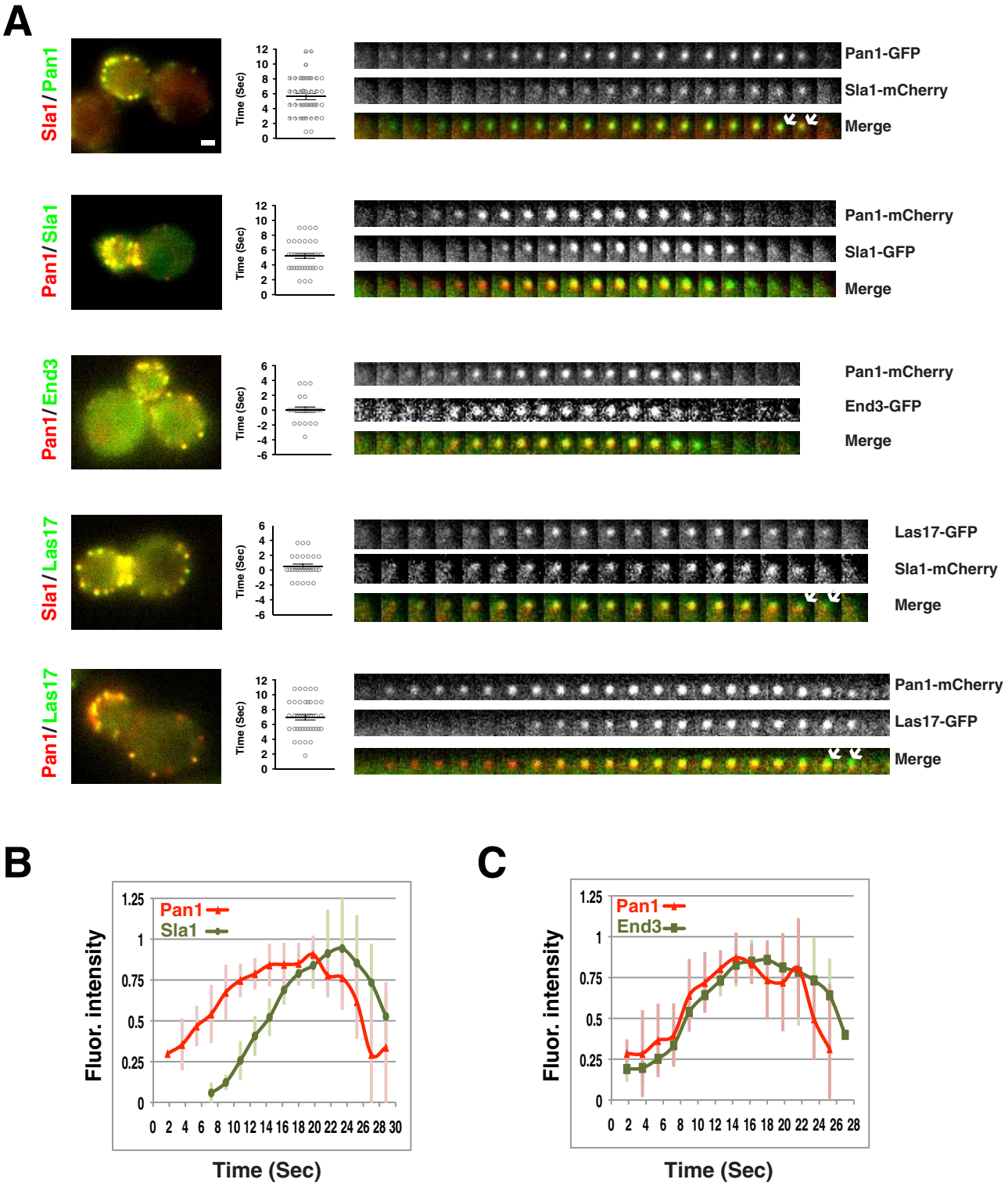

FIGURE 2: Pan1, End3, Sla1 and Las17 recruitment dynamics. (A) Temporal-spatial recruitment of GFP- and mCherry-tagged endocytic patch proteins in live cells. Left, single frames from movies of cells expressing GFP-tagged and mCherry-tagged protein pairs as indicated. Montages, single-channel or merged images, of single patches from two-color movies of cells expressing GFP-tagged and mCherry-tagged proteins as indicated. Time to acquire one image pair is 1.8 s. The plots between the still images and montages show the average arrival time difference (mean ± SD) between the two proteins detected using Icy software (*Materials and Methods*; $n = 30$). The arrows indicate the relative localization of two indicated proteins around the end of their lifetime. (B) Average fluorescence intensity profiles for Pan1-mCherry and Sla1-GFP. GFP and mCherry fluorescence intensities were quantified and plotted for individual endocytic site formation over time ($n = 13$). All of the Sla1 plots were aligned around 50% of the maximum intensity and averaged (mean ± SD). Each individual Pan1-mCherry plot was aligned relative to the simultaneously acquired Sla1 intensity plot, and the Pan1-mCherry plots were averaged (mean ± SD). (C) Average fluorescence intensity profiles of Pan1-mCherry and End3-GFP ($n = 12$). Scale bar, 1 μm.

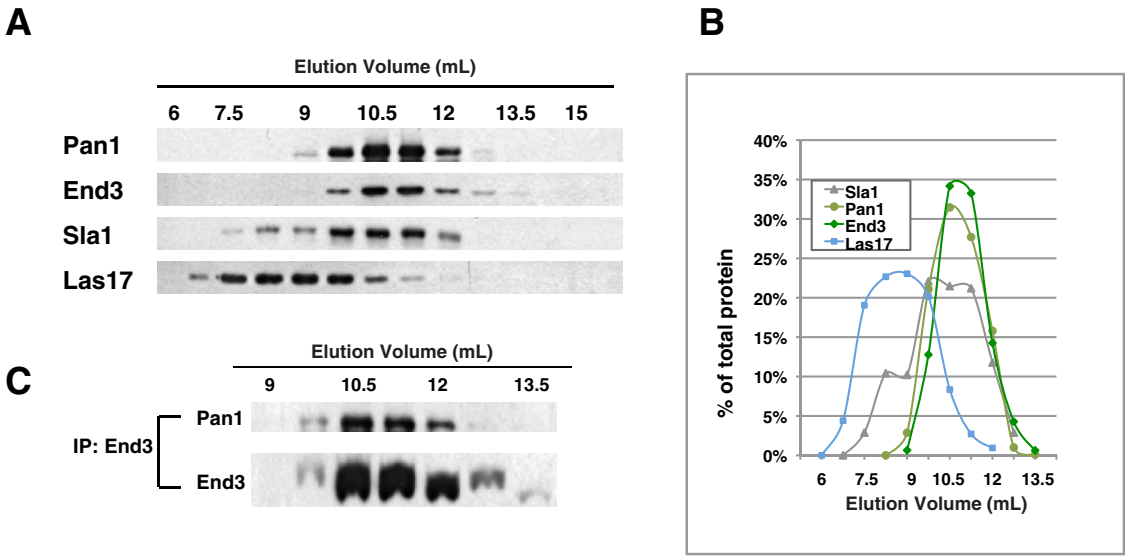

FIGURE 3: Gel filtration analysis of Pan1, End3, Sla1, and Las17. (A) A yeast extract (*MATa ura3-52 leu2-3112 his3Δ200 END3-GFP::HIS3 LAS17-13myc::KanMX6*) was prepared and subjected to gel filtration chromatography as described in *Materials and Methods*. Immunoblot analysis using various antibodies (anti-Pan1, anti-GFP, anti-Sla1, and anti-Myc) detected the indicated proteins in different fractions. (B) Distribution of endocytic proteins in gel filtration fractions. Band intensities for immunoblots shown in A were quantified. For each indicated protein, the band intensity of each fraction was divided by the total band intensity from all fractions. (C) Immunoprecipitation (IP) of End3-GFP using an anti-GFP antibody was performed on the fractions obtained from A, and Pan1 and End3 were detected by immunoblotting.

(Supplemental Figure S2C). Together these results suggest that End3 is recruited into Pan1-containing complexes through the interaction of its C-terminus with Pan1.

The Pan1-End3 complex couples early (coat) module proteins, as well as phosphatidylinositol-4,5-bisphosphate–binding Sla2 and Ent1/2, to the endocytic actin machinery

A recent study using the auxin-inducible degron system to deplete only Pan1 led to the conclusion that Pan1 loss causes a delay in endocytic progression and weakened connections between the coat/actin machinery and the plasma membrane (Bradford *et al.*, 2015). Our results so far demonstrate that Pan1 and End3 show indistinguishable recruitment dynamics in cells and that End3 cortical localization is largely dependent on its association with Pan1, supporting the idea that these two yeast Eps15-like proteins function together as a complex during endocytic internalization. Therefore, rather than investigating Pan1 (Bradford *et al.*, 2015) or End3 individually, we explored the functions of the Pan1-End3 complex by simultaneously eliminating both proteins. To this end, we generated a *PAN1-AID END3-AID TIR1* strain. Immunoblotting confirmed that both Pan1 and End3 are reduced to undetectable levels upon 250 μM auxin treatment for 60–90 min (Supplemental Figure S3A). We analyzed the dynamics of proteins from distinct endocytic modules in *PAN1-AID END3-AID TIR1* cells in the absence (control) or the presence of auxin (Pan1 and End3 depletion). Strikingly, depletion of both Pan1 and End3 caused the actin network to assemble ectopically, uncoupled from the early endocytic module proteins, as will be described further (Figures 5 and 6).

Early and early coat module proteins Ede1 and Apl1, respectively (Carroll *et al.*, 2012), and phosphatiylinositol-4,5-bisphosphate–binding Sla2 and Ent1 still formed cortical patches when Pan1 and End3 were depleted (Figure 5A), indicating that Pan1 and End3 are not required for recruitment or stabilization of these proteins at the cell cortex. However, 90% of Ede1-GFP patches and 94% of Sla2-GFP patches stayed nondynamic (no internalization) in Pan1- and End3-depleted cells for the duration of the movies (Figure 5A and Supplemental Movie S6), indicating a defect in endocytic internalization.

Sla1-GFP dynamics and organization (Figure 5B and Supplemental Movie S7) were dramatically different in cells depleted for both Pan1 and End3 relative to control cells. First, many fewer Sla1-GFP patches were present on the cell cortex when Pan1 and End3 were depleted (91% reduction, from 1.07 ± 0.61 to 0.10 ± 0.07 patches/μm; Figure 5B). Second, Sla1-GFP patches were observed in the cytoplasm, which was not seen in control cells (Figure 5B; Kaksonen *et al.*, 2003). Third, whereas in wild-type cells, Sla1-GFP patches exhibited predictable initial restricted movement followed by a directional movement into the cytoplasm (Figure 5C), as previously described (Kaksonen *et al.*, 2003), in cells depleted for both Pan1 and End3, Sla1-GFP patch dynamics were no longer regular. Some patches moved along the cell cortex in a rapid manner and then disappeared (Figure 5C(1)), whereas others moved rapidly through the cytoplasm at rates and distances far greater than observed in wild-type cells (Figure 5C(2)). In addition, some patches exhibited two phases: a low-motility phase and a high-motility phase (Figure 5C(3)). However, movement during the high-motility phase did not appear to be directed toward the cell center (Figure 5C(3)).

Sla1 dynamics in cells depleted for both Pan1 and End3 was different from the dynamics in cells depleted for only Pan1 (Bradford *et al.*, 2015) or only End3. In the cells depleted for either Pan1 or End3 alone, the number of Sla1-GFP patches on the cell cortex was reduced by 58% (from 1.50 ± 0.54 to 0.64 ± 0.13 patches/μm) and 52% (from 1.42 ± 0.27 to 0.68 ± 0.14 patches/μm), respectively, and correspondingly more Sla1-GFP was diffuse in the cytoplasm (Supplemental Figure S3B). However, Sla1-GFP patches detected in cells depleted for only Pan1 or only End3 were present on the cell cortex

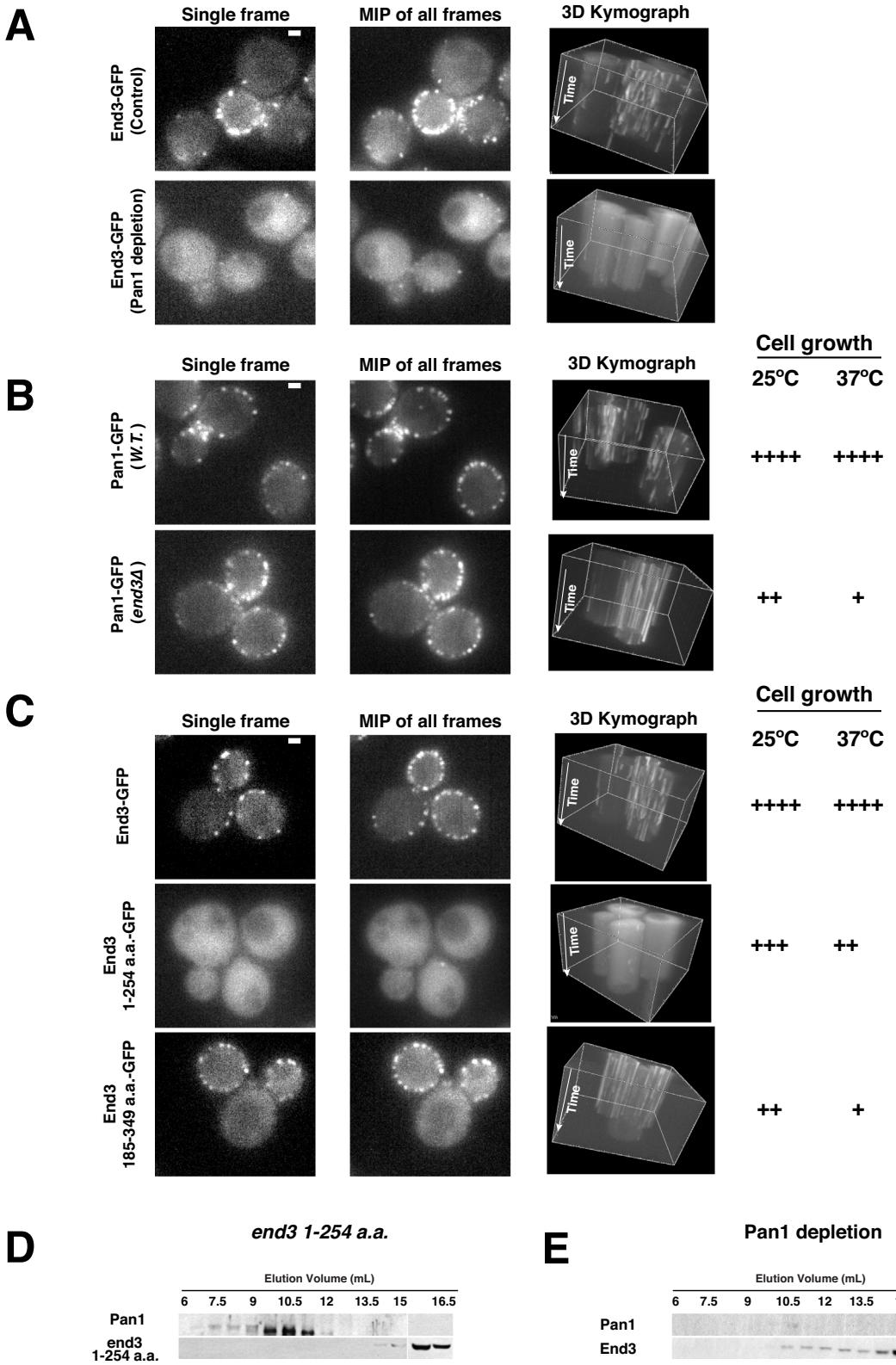

FIGURE 4: Pan1 recruits End3 to endocytic sites through its interaction with the End3 C-terminus. (A) End3-GFP patch dynamics in Pan1-depleted cells. *END3-GFP PAN1-AID TIR1* cells were treated with 250 μM auxin or DMSO (control) for 60 min and then imaged by epifluorescence microscopy. Left, single frames (1 s/frame) from 2-min movies of indicated cells. Middle, maximum intensity projections (MIPs) of all frames from the 2-min movies, showing the total number of endocytic sites generated during the 2-min movies. Right, three-dimensional (3D) kymographs generated by Imaris software from the 2-min movies. (B) Pan1-GFP patch dynamics in wild-type or *end3Δ* cells. Single frames (1 s/frame), MIPs, and 3D kymographs were generated from 2-min movies as indicated. Growth phenotypes for each strain are indicated. (C) Patch dynamics for End3-GFP, End3 1-254 a.a.–GFP, and End3 185-349 a.a.–GFP. Single frames

(Supplemental Figure S3B), and ~60–70% of the cortical patches no longer moved inward and were present for longer times (Supplemental Figure S3B; Bradford *et al.*, 2015), suggesting that endocytic internalization is impaired. These results suggest that Pan1 and End3 share functions in recruiting Sla1-GFP to the cell cortex and restricting its movement.

Previously we showed that Sla1 is recruited to Sla2 patches ~10 s after Sla2 arrives and then shares similar behavior with Sla2 for ~30 s during the lifetime of the Sla1 patch (Carroll *et al.*, 2012). However, in cells depleted for both Pan1 and End3, we observed that Sla2-GFP patches stay nonmotile at the cell cortex (Figure 5A), whereas Sla1-GFP patches move dynamically either near the cell cortex or through the cytoplasm (Figure 5B), indicating that Sla1 and Sla2 are no longer present in the same patches. For further confirmation of this observation, we performed two-color live-cell imaging of *PAN1-AID END3-AID TIR1* cells expressing Sla1-GFP and Sla2-TagRFP-T in the absence or presence of 250 μM auxin. When Pan1 and End3 were depleted, 90% of the Sla2-TagRFP-T patches did not contain Sla1-GFP for the duration of the 1.8-min movies (Figure 5D and Supplemental Movie S8). In addition, most of the cortical Sla1 patches did not contain Sla2-TagRFP-T (Figure 5D and Supplemental Movie S8). Taken together, these results indicate that Sla1 no longer associates with Sla2 patches when Pan1 and End3 are both depleted.

Endocytic actin dynamics was analyzed by imaging actin-binding protein 1 (Abp1)–red fluorescent protein (RFP) in cells lacking Pan1 and End3. In control cells, Abp1-RFP patches form at the cell cortex and move a short distance into the cytoplasm (Kaksonen *et al.*, 2003; Figure 5E and Supplemental Movie S9). Surprisingly, in cells depleted for both Pan1 and End3, Abp1-RFP formed comet tail–like structures instead of patches, either near the cell cortex or in the cytoplasm, moving dynamically in an apparently random manner with trajectories similar to those of Sla1 patches (Figure 5, B and E, and Supplemental Movie S9). We found that the frequency of actin tail formation is much higher in Pan1- and End3-depleted cells (88% of cells showed at least one actin tail during the duration of a 1.8-min movie) than in Pan1-depleted cells (12%) or in End3-depleted cells (1.6%). Similar results were obtained when Sac6 (yeast fimbrin)-RFP was used as an actin marker. Two-color live-cell imaging was performed on *PAN1-AID END3-AID TIR1* cells expressing both Sla1-GFP and Abp1-RFP in the absence and presence of 250 μM auxin. In control cells, Abp1-RFP was recruited to cortical Sla1 patches and disappeared soon after Sla1-GFP (Figure 6A and Supplemental Movie S10). Strikingly, in cells depleted for both Pan1 and End3, Sla1-GFP patches associated with the leading tip of Abp1-RFP comet tails, moving dynamically through the cytoplasm (Figure 6A and Supplemental Movie S11) or moving to and/or sliding along the cell cortex (Supplemental Movie S11). Thus the Sla1 patches seem to be propelled by assembly of an actin tail in a manner similar to movement of *Listeria* intracellular pathogens (Welch and Way, 2013). In contrast, in the cells depleted for Pan1 or End3 alone, the Sla1-GFP patches were mostly restricted to the cell cortex and recruited Abp1-RFP before disappearing (Supplemental Figure S3, C and D; Bradford *et al.*, 2015).

We also examined the localization of GFP-tagged proteins in the WASP/MYOSIN module (Las17, Vrp1, Myo5, and Bbc1) and AMPHIPHYSIN module (Rvs167) in cells lacking both Pan1 and End3, using Abp1-RFP as a reference. Of interest, when Pan1 and End3 are depleted from cells, all of the proteins in these two modules behaved similarly to Sla1, localizing at the leading tip of the Abp1-RFP comet tails (Figure 6B and Supplemental Movies S10 and 12). In contrast, neither Ede1-GFP nor Sla2-GFP associated with the actin comet tails (Supplemental Figure S4).

The foregoing results are summarized in Figure 6C. In the absence of the Pan1-End3 complex, the early and early coat module proteins, as well as Sla2, Ent1, and Ent2, still assemble at cortical sites, and the endocytic actin network still assembles. However, the actin network does not assemble in association with the early endocytic proteins in cells depleted of Pan1 and End3. Taken together, our results demonstrate that the endocytic actin network can assemble independently of the early and early coat module proteins Sla2/Ent1/2, and Pan1 and End3 in vivo. Moreover, our data establish that Pan1 and End3 together play a key role in endocytic-site maturation by coupling actin assembly to endocytic sites.

Sla1 was shown to play a role in Las17 recruitment (Rodal *et al.*, 2003; Feliciano and Di Pietro, 2012), which is critical for assembly of the endocytic actin network (Sirotkin *et al.*, 2005; Sun *et al.*, 2006). Thus Pan1-End3 likely recruits actin assembly machinery to endocytic sites at least partially through interactions with Sla1. To gain mechanistic insights into how the Pan1-End3 complex is involved in cortical recruitment of Sla1, we generated Pan1 or/and End3 truncation mutants lacking only the previously identified Sla1-binding regions (Tang *et al.*, 2000; Figure 1C).

As shown in Figure 6D, Sla1-GFP cortical localization is severely diminished in an *end3* truncation mutant lacking the first 185 a.a. *(end3 1-185 del)* but not in *pan1 98-385 a.a. del* cells. These results suggest that the End3-Sla1 interaction plays a major role in Sla1 recruitment. In addition, a *pan1 98-385 a.a. del end3 1-185 a.a. del* double mutant is lethal at 37°C and grows much more poorly than *pan1 98-385 a.a. del* and *end3 1-185 a.a. del* single mutants at room temperature (Figure 6D and Supplemental Figure S5A), suggesting that Pan1 plays a supportive role with End3 in Sla1 recruitment. In contrast, in *sla1Δ* cells, both Pan1-mCherry and End3-GFP still appear at the cell cortex and then move inward (Supplemental Figure S5B). Thus Sla1 is not required for Pan1 or End3 recruitment.

The Sla1 N- and C-termini can be recruited to endocytic sites independently

The C-terminal region of Sla1 interacts with Pan1 and End3 in vitro (Tang *et al.*, 2000; Figure 1C). Thus we next determined whether this C-terminal region is sufficient to localize Sla1 to endocytic sites. As shown in Figure 7A, Sla1 850-1244 a.a.–GFP patches appear at the cell cortex and then move off the cortex with a much longer lifetime (149 ± 45 s) than Sla1-GFP (Figure 7A and Supplemental Movie S13), presumably due to partial loss of Sla1 function. In addition, Sla1 850-1244 a.a.–GFP no longer localizes to the cell cortex in cells depleted for both Pan1 and End3 (Supplemental Figure 6A), indicating that Sla1 850-1244 a.a.–GFP cortical localization is dependent on Pan1 and End3.

Of interest, GFP-tagged Sla1 N-terminal region was reported to localize both on the cell cortex and in the nucleus (Chi *et al.*, 2012), implying that the Sla1 C-terminal region may not be the only region involved in Sla1's cortical localization. Hence we generated a

(1 s/frame), MIPs, and 3D kymographs were generated from 2-min movies as indicated. End3-GFP, End3 1-254 a.a.–GFP, and End3 185-349 a.a.–GFP were expressed at similar levels (Supplemental Figure S2). Growth phenotypes for each strain are indicated (Supplemental Figure S2). (D, E). Gel filtration analysis of yeast cell extracts. Yeast extracts were prepared from *end3 1-254 a.a.* or Pan1-depleted cells. Scale bars, 1 μm.

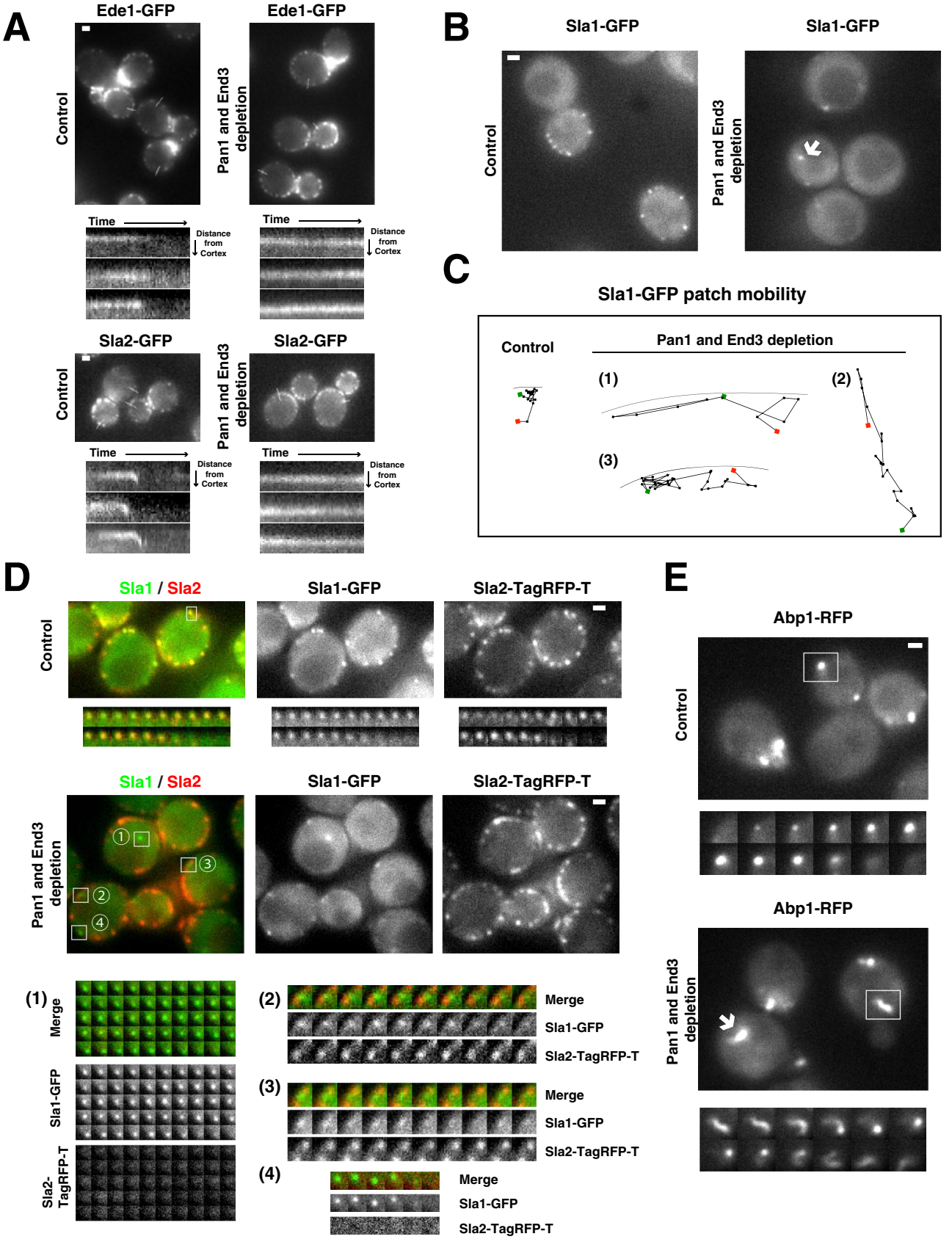

FIGURE 5: Dynamics of endocytic patch proteins in Pan1/End3 double-depleted cells. *PAN1-AID END3-AID TIR1* cells expressing GFP-tagged and/or RFP-tagged proteins were observed. Pan1 and End3 were depleted from the cells by adding 250 μM auxin for 60–90 min before observation. (A) Dynamics of Ede1-GFP and Sla2-GFP patches. The cell images are single frames from 1.8-min movies as indicated. Kymographs of individual patches were generated from the

sla1 1-855 a.a.–GFP strain. Consistently, Sla1 1-855 a.a.–GFP showed both cortical and nuclear localization (Figure 7A; Chi *et al.*, 2012). The nuclear localization of Sla1 1-855 a.a.–GFP is likely due to nuclear localization sequences (Gardiner *et al.*, 2007). We focused our studies on the nature of the cortical Sla1 1-855 a.a.–GFP patches and how they are related to endocytic sites.

Kymograph analysis revealed that Sla1 1-855 a.a.–GFP does not move inward, which is different from the behavior of Sla1-GFP and Sla1 855-1244 a.a.–GFP (Figure 7A and Supplemental Movie S13). Intriguingly, we found that Sla1 1-855 a.a.–GFP localizes to the cell cortex even in cells depleted for both Pan1 and End3 (Supplemental Figure S6B). Thus cortical localization of Sla1 1-855 a.a.–GFP is not dependent on Pan1 or End3, indicating that the Sla1 N-terminus contains a cryptic endocytic binding site.

We further investigated the spatial relationship of Sla1 1-855 a.a.–GFP to other endocytic proteins labeled with mCherry or RFP. As shown in Figure 7B, Sla1 1-855a.a.–GFP colocalizes with Ede1-mCherry at the cell cortex, indicating that Sla1 1-855 a.a.–GFP localizes at endocytic sites. Of importance, in *sla1 1-855 a.a.–GFP* cells, when Pan1-mCherry, Sla2-TagRFP-T, Rvs167-RFP, or Sac6-RFP moved inward at the end of its lifetime, Sla1 1-855 a.a.–GFP remained nonmotile at the cell cortex (Figure 7C and Supplemental Movie S14). Because such inward movement is believed to represent membrane invagination and vesicle formation (Kaksonen *et al.*, 2003), our results imply that Sla1 1-855 a.a.–GFP becomes physically separated from Pan1, Sla2, Sac6, and Rvs167 at this stage (Figure 7E). Thus Sla1 1-855 a.a.–GFP, which cannot interact with Pan1 or End3, fails to exhibit the same dynamic behavior as Pan1-End3 during endocytic vesicle formation.

We also generated a strain that expresses both Sla1 1-855 a.a.–GFP (at the native *SLA1* locus) and Sla1 850-1244 a.a.–mCherry (at the *URA3* locus). As shown in Figure 7D, Sla1 1-855 a.a.–GFP localized to both the cell cortex and the nucleus, whereas Sla1 850-1244 a.a.–mCherry was at patches at the cell cortex (Supplemental Movie S15). Strikingly, clear spatial separation was observed between Sla1 1-855 a.a.–GFP, which remained at the cell cortex, and Sla1 850-1244 a.a.–mCherry, which moved into the cell, at the moment patches moved off cell cortex (membrane invagination; Figure 7, D and E). Of interest, similar to an *sla1Δ* strain, this *sla1 1-855 a.a.–GFP sla1 850-1244 a.a.–mCherry* strain is dead at 39°C (Figure 7E), indicating that the N- and C-termini of Sla1 must be physically linked for Sla1 to function correctly, even though they can associate with endocytic sites independently.

Sla1 carries the pheromone receptor Ste2 into endocytic vesicles through interaction of its C-terminus with Pan1-End3

The foregoing results demonstrate that the N- and C-termini of Sla1 are recruited to endocytic sites in a Pan1-End3–independent and –dependent manner, respectively. In *end3 1-185 a.a. del pan1 98-385 a.a. del* double-mutant cells, the Sla1 C-terminus can no longer interact with Pan1 or End3 because the Sla1-binding domains of Pan1 and End3 are truncated. Because the Sla1 N-terminus can be recruited to the cell cortex independently of the C-terminus (Figure 7A), one might expect that Sla1-GFP in the *end3 1-185 a.a. del pan1 98-385 a.a. del* double-mutant cells would display localization similar to sla1 1-855 a.a.–GFP. However, in *end3 1-185 a.a. del pan1 98-385 a.a. del* double-mutant cells, Sla1-GFP loses most of its cortical localization (Figure 6D). In addition, unlike in *sla1 1-855 a.a.–GFP* mutant cells, the Sla1-GFP signal is not detected in the nucleus in the *end3 1-185 a.a. del pan1 98-385 a.a. del* double-mutant strain (Figures 6D and 7A). These results lead us to conclude that full-length Sla1 localizes to endocytic sites primarily through interaction of its C-terminal region with Pan1-End3.

We next addressed how and why the Sla1 N-terminal region alone localizes to the cell cortex. Sla1 1-855 a.a. contains three SH3 domains followed by an Sla1 homology domain 1 (SHD1), an Sla1 homology domain 2 (SHD2), and a clathrin box motif (CBM; Figure 8A). We examined which of these domains is responsible for the cortical localization of Sla1 1-855 a.a.–GFP (Figure 8B). Our data indicate that SHD2 and CBM are not required for Sla1 cortical localization (Figure 8B), because a fragment containing Sla1 1-650 a.a.–GFP was sufficient for cortical localization. A few Sla1 1-480 a.a.–GFP patches appear on the cell cortex in a pattern that is very different from the pattern for Sla1 1-650 a.a.–GFP patches, suggesting that the SHD1 region plays a key role in Sla1 1-855 a.a.–GFP cortical localization (Figure 8B). Intriguingly, Sla1 was shown to serve as a cargo adaptor through this SHD1 region, which specifically binds to endocytic receptors containing the NPFXD internalization signal (Howard *et al.*, 2002). Thus these results imply that Sla1 1-855 a.a.–GFP is recruited to the cell cortex through interaction of its SHD1 domain with endocytic cargo proteins.

On the basis of our results, we speculate that Sla, Pan1, and End3 may function as follows. Pan1-End3 facilitates Sla1 recruitment to cortical patches through interactions with the Sla1 C-terminus (Figure 6D). When it arrives at endocytic sites, the Sla1 N-terminus interacts with NPFXD-containing endocytic cargo proteins. The Pan1-End3 complex then pulls Sla1 and its associated endocytic cargo proteins into endocytic vesicles.

To further test our idea, we examined Ste2 NPFXD-GFP localization in both wild-type and *sla1 1-855 a.a.* cells (Figure 8C). *STE2* encodes the α-factor pheromone receptor. Ste2 can be internalized by both ubiquitin-dependent and NPFXD-dependent endocytosis (Howard *et al.*, 2002). However, *ste2 NPFXD* is a *ste2* mutant that can only be internalized through binding of its NPFXD sequence to the Sla1 SHD1 domain (Howard *et al.*, 2002). In wild-type cells, Ste2 NPFXD-GFP was internalized to the vacuole (Figure 8C). Strikingly, in *sla1 1-855 a.a.* cells, Ste2 NPFXD-GFP localized only at the cell cortex (Figure 8C). One possibility was that the block of Ste2 NPFXD-GFP internalization in the *sla1 1-855 a.a.* mutant was due to a bulk endocytic deficiency, which may be caused by partial loss of Sla1 function. This is unlikely, however, because wild-type Ste2-GFP

movies using ImageJ software. Interval between frames is 1.8 s. (B, C) Particle tracking of individual Sla1-GFP patches. The cell images are single frames from 1.8-min movies as indicated. Interval between frames is 1.8 s. Arrow points to a patch localized in the cytoplasm. Particle tracking analysis was performed on the indicated movies using Icy software. Green and red dots denote the first and last positions, respectively, of each patch. (D) Sla1-GFP and Sla2-TagRFP-T patch dynamics. The cell images are single frames from 1.8-min movies as indicated. The montages, single-channel or merged images, of single patches from two-color movies of cells expressing both Sla1-GFP and Sla2-TagRFP-T. Time to acquire one image pair is 1.8 s. (E) Abp1-RFP dynamics. The cell images are single frames from 1.8-min movies as indicated. Montages of single patches from movies as indicated. Interval between frames is 1.8 s. The arrow points out one actin tail localized in the cytoplasm. Scale bars, 1 μm.

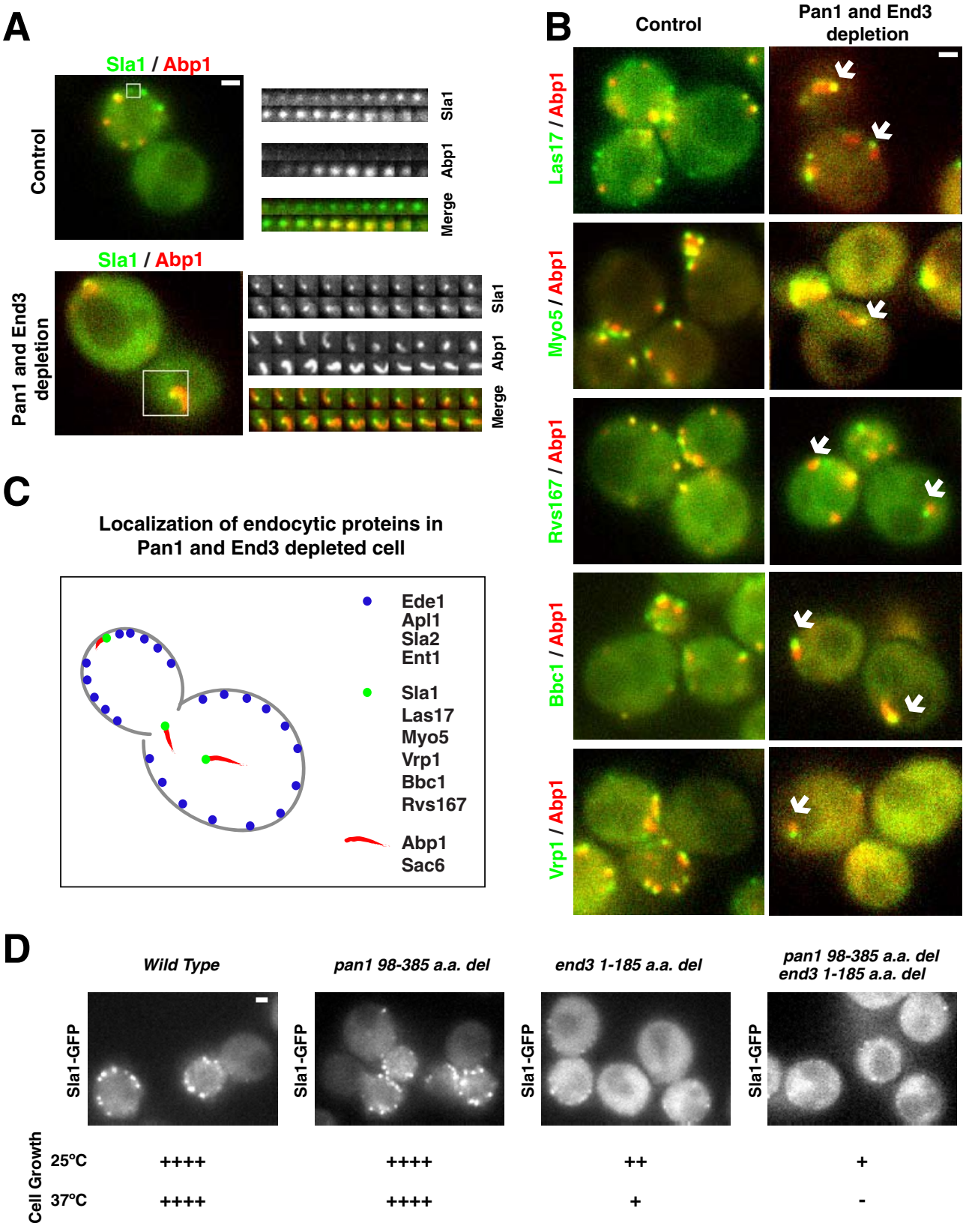

FIGURE 6: Pan1 and End3 function together to couple early (coat) module proteins, as well as Sla2 and Ent1/2, to the endocytic actin machinery. *Pan1-AID End3-AID- TIR1* cells expressing GFP-tagged and/or RFP-tagged proteins were observed. Pan1 and End3 were depleted from the cells by adding 250 μM auxin for 60–90 min before observation. (A) Sla1-GFP and Abp1-RFP patch dynamics. Montages, single-channel or merged images, of single patches from two-color movies of cells expressing both Sla1-GFP and Abp1-RFP. Time to acquire one image pair is 1.8 s. (B) Localization of Abp1-RFP and a GFP-tagged patch protein in living cells. Each image is a single frame from a

can still be internalized in *sla1 1-855 a.a.* cells (Figure 8C), presumably through a ubiquitin-dependent pathway by other adapters. Thus our results strongly support a model in which Sla1 pulls NPFXD-containing endocytic protein cargo into endocytic vesicles via interaction between the Sla1 C-terminus and Pan1-End3.

DISCUSSION

Molecular basis for coordination between receptors, adaptors, and actin assembly at endocytic sites

Our study revealed mechanistic details of the dynamic interactions and functions of Pan1, End3, and Sla1. On the basis of our results, we propose that Pan1, End3, and Sla1 coordinate cargo capture with actin assembly at endocytic sites, as described below (see discussion of Figure 9).

Observations reported here and elsewhere provide clarity to the order of endocytic protein recruitment and the underlying interactions. Pan1 and End3 coexist in a stable complex (Figures 2 and 3) and are recruited to the endocytic site after the early module proteins, early coat module proteins, and phosphatidylinositol-4,5-bisphosphate–binding Sla2/Ent1/2. Sla2 and Ent1 are likely to play roles in recruiting Pan1 and End3 to endocytic sites, since Sla2 and Ent1 were previously shown to interact with Pan1 and End3 (Wendland and Emr, 1998; Toshima *et al.*, 2007; Boeke *et al.*, 2014). The End3 C-terminus is necessary and sufficient for End3 recruitment to endocytic sites by Pan1 (Figure 4). Sla1 appears to be recruited next through interaction of its C-terminus with the Pan1-End3 complex (Figures 6D and 7A). End3 plays a crucial role, whereas Pan1 plays an apparently redundant role, in Sla1 recruitment (Figure 6D). Las17 is recruited to endocytic sites partially through its interaction with Sla1 (Figure 2A; Feliciano and Di Pietro, 2012). Sla1 inhibits Las17's actin nucleation activity before these proteins arrive at endocytic sites (Rodal *et al.*, 2003; Feliciano and Di Pietro, 2012). Once Sla1 arrives at endocytic sites, its N-terminus interacts with NPFXD motif–containing endocytic cargo receptors (Figure 8). Las17 serves as a key scaffold and activator of actin assembly (Sirotkin *et al.*, 2005; Sun *et al.*, 2006), which generates force to induce membrane invagination and constriction. Our results indicate that the Pan1-End3 complex then pulls Sla1 to the bottom of the invaginated pit, whereas Las17 is left at the base and/or along the tubule (Figure 2A). The physical separation of Sla1 and Las17 may lead to a complete release of Sla1's inhibition of Las17's actin nucleation–promoting activity, further facilitating endocytic vesicle formation. Meanwhile, Sla1 pulls NPFXD motif–containing endocytic cargo into the forming vesicle. As such, the Pan1-End3 complex plays a key role in endocytic-site formation and maturation, at least partially by recruiting Sla1 and Las17, to ensure that cargo capture occurs coordinately with endocytic actin assembly. Moreover, the conservation of these proteins suggests that similar mechanisms may operate in all eukaryotes.

When Pan1 and End3 are depleted from the cell, the early (coat) module proteins and Sla2/Ent1/2 are still able to establish cortical patches (Figures 5A and 9), and actin is able to assemble (Figures 5E, 6, and 9). However, without Pan1 and End3, the endocytic actin network no longer associates with the early (coat) module proteins and Sla2/Ent1/2 (Figures 5, 6, and 9 and Supplemental Figure S4), indicating that the Pan1-End3 complex is crucial to couple actin assembly to endocytic sites.

Interaction of the Pan1-End3 complex with the C-terminus of Sla1 plays a key role in the initial recruitment of Sla1 to endocytic sites (Figures 6D and 7A) and in attaching Sla1 to the forming endocytic vesicle (Figure 8). Without its C-terminal region, Sla1 1-855–GFP localizes to endocytic sites, likely through the interaction of its SHD1 domain with NPFXD motif–containing endocytic cargo proteins (Figure 8B). However, Sla1 1-855–GFP is not recruited to the invaginated endocytic membrane, since it cannot interact with the Pan1-End3 complex (Figure 7C). Therefore, in *sla1 1-855* cells, NPFXD motif–containing endocytic receptors are stuck at the plasma membrane and are not internalized (Figures 8C and 9).

Rethinking the early and late phases of endocytic internalization

Endocytic internalization has been described as consisting of an early and a late phase mainly based on protein recruitment order and lifetime regularity (Carroll *et al.*, 2012; Brach *et al.*, 2014). However, the functional logic underlying the "early- and late-phase" organization of the CME pathway was not clear. In our study, upon rapid and simultaneous elimination of both Pan1 and End3, proteins from different endocytic modules segregated into two distinct cellular locations (Figure 6C). This unique and profound phenotype led us to rethink CME phase organization from a functional perspective.

Recent studies established that Sla2 and Ent1/2 appear at endocytic sites before Pan1 and End3 (Carroll *et al.*, 2012; Brach *et al.*, 2014). Consistently, we showed that Sla2 and Ent1 cortical localization are independent of Pan1 and End3 (Figure 5A). Moreover, a previous study showed that Sla2 and Ent1 can initiate endocytic sites in the absence of several early and early coat module proteins (Brach *et al.*, 2014). Based on these functional findings, Sla2 and Ent1/2 appear to belong to the same phase as the early module and early coat module proteins (Figure 9). Thus we propose that endocytic internalization consists of two functional phases: the "endocytic-site initiation phase," during which the early module, early coat module, and Sla2/Ent1/2 are recruited, and the "actin assembly phase," during which the WASP/MYOSIN, AMPHIPHYSIN, and ACTIN modules are recruited (Figure 9). By eliminating both Pan1 and End3 from cells, we demonstrated that endocytic-site initiation and endocytic actin machinery assembly are mechanistically independent processes coupled by the Pan1-End3 complex (Figures 5 and 6).

A recent study on cells depleted for only Pan1 reported that few cortical actin patches form, and some of them turn into "actin flares" (Bradford *et al.*, 2015). The actin flares were reported to originate at cortical endocytic patches and to extend into the cytoplasm (Bradford *et al.*, 2015). The coat components Sla2, Sla1, and End3 moved with the tip of the actin flare (Bradford *et al.*, 2015). In our study, we depleted Pan1 and End3 simultaneously and observed a pronounced presence of actin comet tails, whose anatomy and biochemical makeup are depicted in Figure 6C. How these actin comet

two-color movie of cells expressing Abp1-RFP and a GFP-tagged protein as indicated. The arrows indicate that the GFP-tagged protein associates with one end of the Abp1-RFP labeled actin comet tail. (C) Summary of endocytic protein localization in Pan1- and End3-depleted cells. The proteins in green associated with the tip of the actin comet tails, but not along the comet tails. See text for detailed description. (D) Cortical localization of Sla1 is dependent on End3 and Pan1. Sla1-GFP localization was examined in *pan1* and *end3* mutants as indicated. The cell growth phenotypes of the strains are indicated (Supplemental Figure S5). Scale bars, 1 μm.

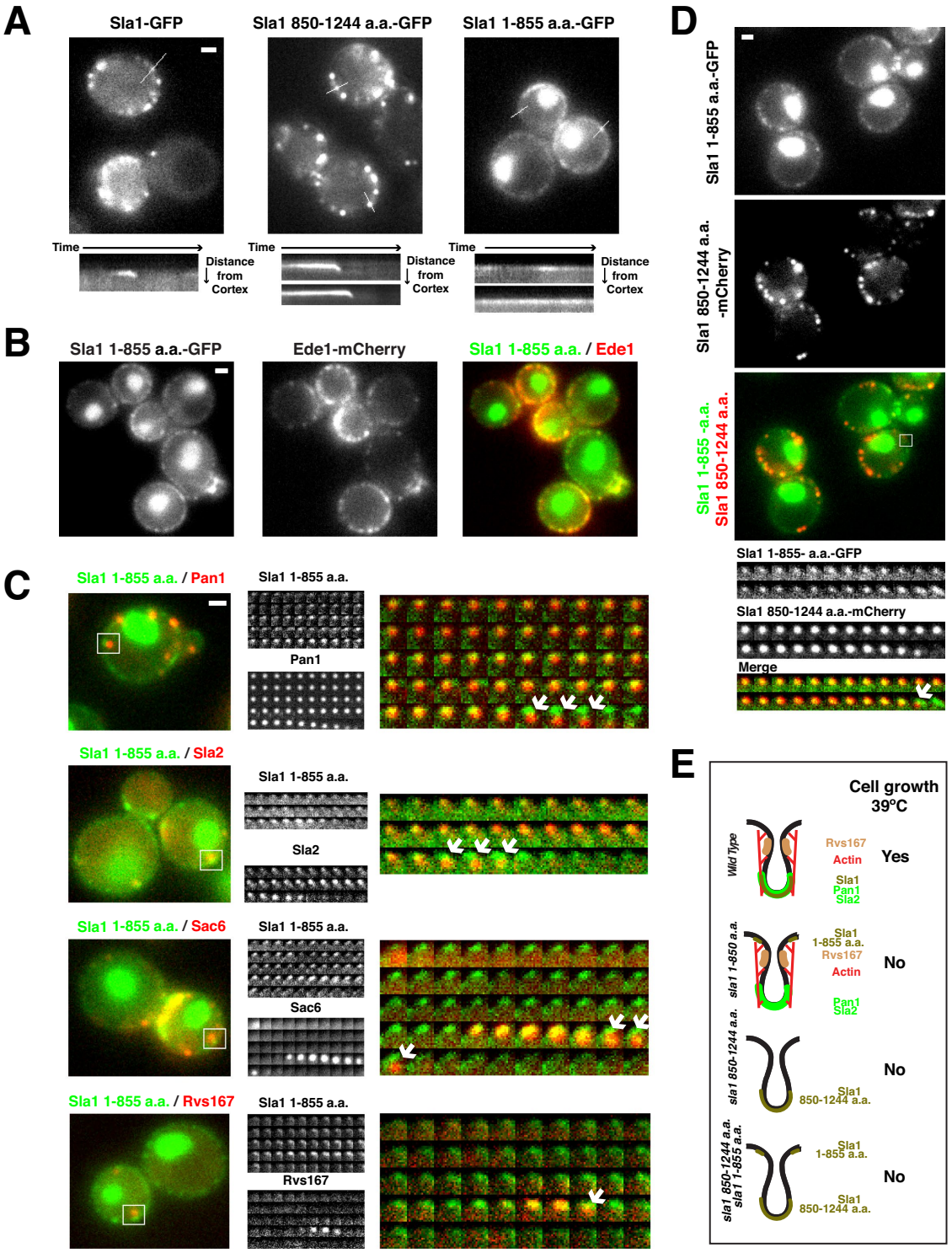

FIGURE 7: Sla1's N-terminus and C-terminus can be recruited to endocytic sites independently. (A) Patch dynamics of Sla1-GFP, Sla1 850-1244 a.a.–GFP, and Sla1 1-855 a.a.–GFP. The cell images are single frames (1 s/frame) from 2-min movies as indicated. Kymographs of individual patches were generated from the 2-min movies using ImageJ software. (B) Localization of Ede1-mCherry and Sla1 1-855 a.a.–GFP in live cells. (C) Patch dynamics of Sla1 1-855 a.a.–GFP and RFP-tagged proteins. The montages, single-channel or merged images, of single patches from two-color movies as indicated. Time to acquire one image pair was 1.8 s. The arrows point out the spatial separation of two indicated proteins. (D) Dynamics of Sla1 1-855 a.a.–GFP and Sla1 850-1244 a.a.–mCherry in living cells. The montages, single-channel or merged images, of a single patch from two-color movies of cells expressing Sla1 850-1244 a.a.–GFP and Sla1 850-1244 a.a.–mCherry. Time to acquire one image pair was 1.8 s. The arrow indicates the spatial separation of Sla1 850-1244 a.a.–GFP and Sla1 850-1244 a.a.–mCherry at the end of their lifetimes. (E) Proposed localization of various Sla1 mutant proteins on the invaginated endocytic membrane. Cell growth phenotypes for *sla1* mutants are summarized. Scale bars, 1 μm.

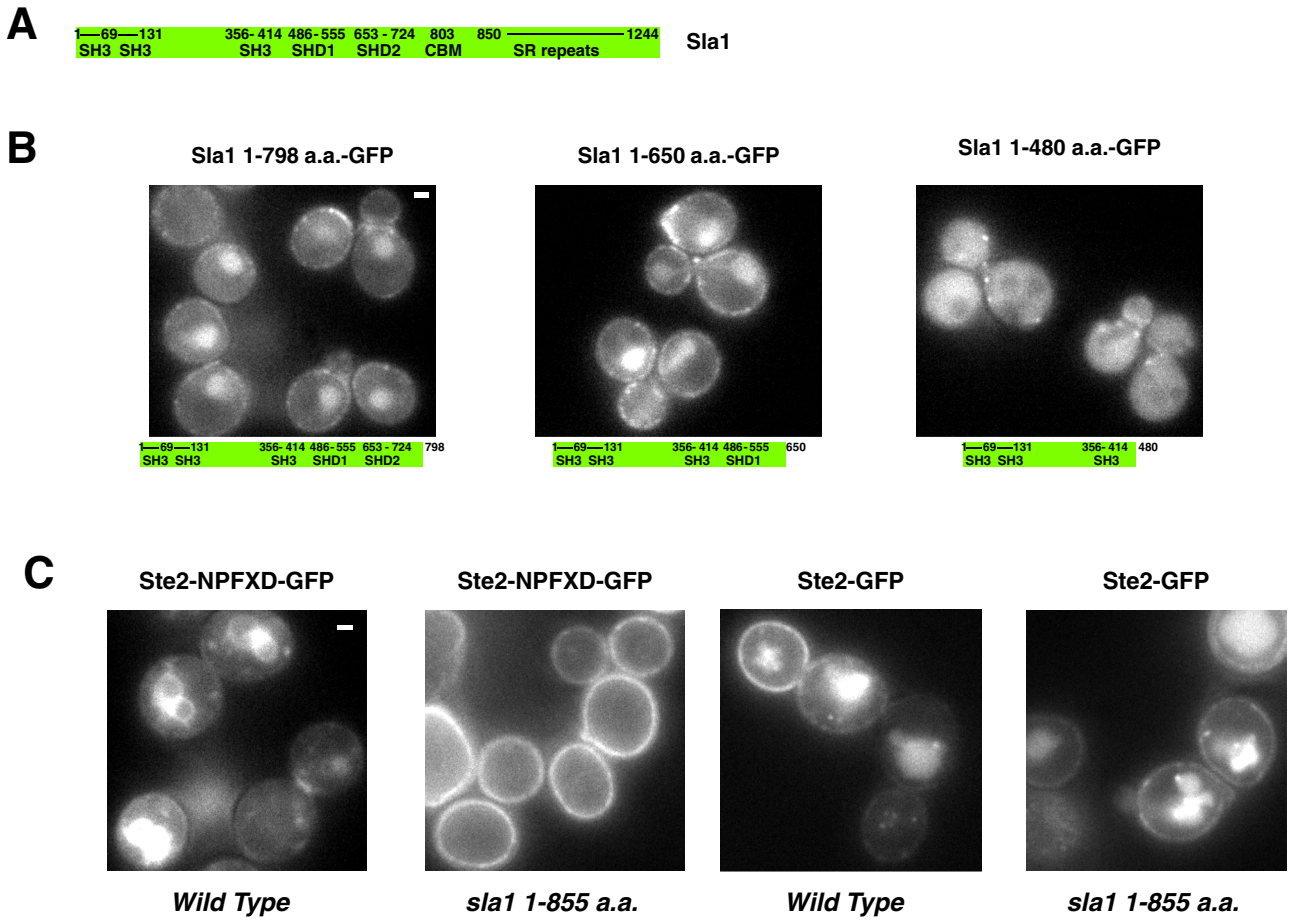

FIGURE 8: SHD1 domain plays key roles in Sla1 1-855 a.a.–GFP cortical localization, and Ste2 NPFXD-GFP cannot be internalized in *sla1 1-855 a.a.* cells. (A) Sla1 domain structure. CBM, clathrin box motif; SH3, Src homology 3; SHD1, Sla1 homology domain 1; SHD2, Sla1 homology domain 2; SR repeats, LxxQxTG repeats. (B) Localization of GFP-tagged Sla1 mutant proteins. (C) Localization of Ste2 NPFXD-GFP or Ste2-GFP in wild-type or *sla1 1-855 a.a.* cells. Scale bars, 1 μm.

tails originated is not clear because of their complex three-dimensional dynamics. However, Sla2 and Ent1/2 remained at the cell cortex and were not observed to associate with the actin comet tails in cells depleted for Pan1 and End3 (Figure 5, A and D, and Supplemental Figure S4), consistent with the notion that early and late endocytic phases had been uncoupled.

Why is a two-phase design used in endocytic-site formation? In yeast, endocytic actin assembly provides the key force for clathrin-mediated endocytic vesicle formation. The mechanistic independence of endocytic-site initiation and actin assembly provides an explanation for the diversity of force generation systems that have evolved for different types of endocytosis in various species (Doherty and McMahon, 2009) and also reflects the ability of the actin machinery to be adopted by diverse cellular processes through evolution (Goley and Welch, 2006).

Dynamic interaction of Pan1, End3, and Sla1 during endocytic vesicle formation

Earlier studies of Pan1, End3, and Sla1 identified the domains responsible for their physical interactions in vitro (Tang *et al.*, 2000). Mass spectrometry analysis of proteins associated with purified TAP-tagged Pan1 suggested that it forms a stable complex with End3 but not with Sla1 (Toshima *et al.*, 2007). These previous studies raised important questions. When and where do these three proteins interact within the cell? How do these interactions affect the functions of Pan1, End3, and Sla1 in vivo?

In this study, gel filtration and live-cell imaging experiments demonstrated that Pan1 and End3, but not Sla1, are stably associated and exhibit indistinguishable dynamic behavior at endocytic sites. Consistently, a recent fluorescence cross-correlation spectroscopy study suggested that Pan1 interacts with End3 in the cytoplasm with a high affinity (K_d < 150 nM) in live cells (Boeke *et al.*, 2014). That study did not detect significant interactions between Sla1 and Pan1 (or End3) in the cytoplasm. These results implied that the binding affinity of Sla1 for Pan1 (or End3) in the cytoplasm is rather low and/or the interaction is very transient. Sla1 may only interact with the Pan1-End3 complex at endocytic sites, when Pan1-End3 complex local concentration is high. Our live-cell imaging analysis supports this notion, as Sla1 patches initiate at endocytic sites after Pan1 and End3 have reached >50% of their maximum recruitment (Figure 2).

In *end3 1-185 a.a. del pan1 98-385 a.a. del* double-mutant cells, cortical localization of full-length Sla1 was mostly lost, and it did not localize in the nucleus (Figure 6D). Thus, when the Sla1 C-terminus cannot interact with the Pan1-End3 complex, the Sla1 N-terminus appears to be unable to mediate its cortical or nuclear localization. A possible explanation for this observation is that in the absence of an interaction with the Pan1-End3 complex at the cell cortex, the

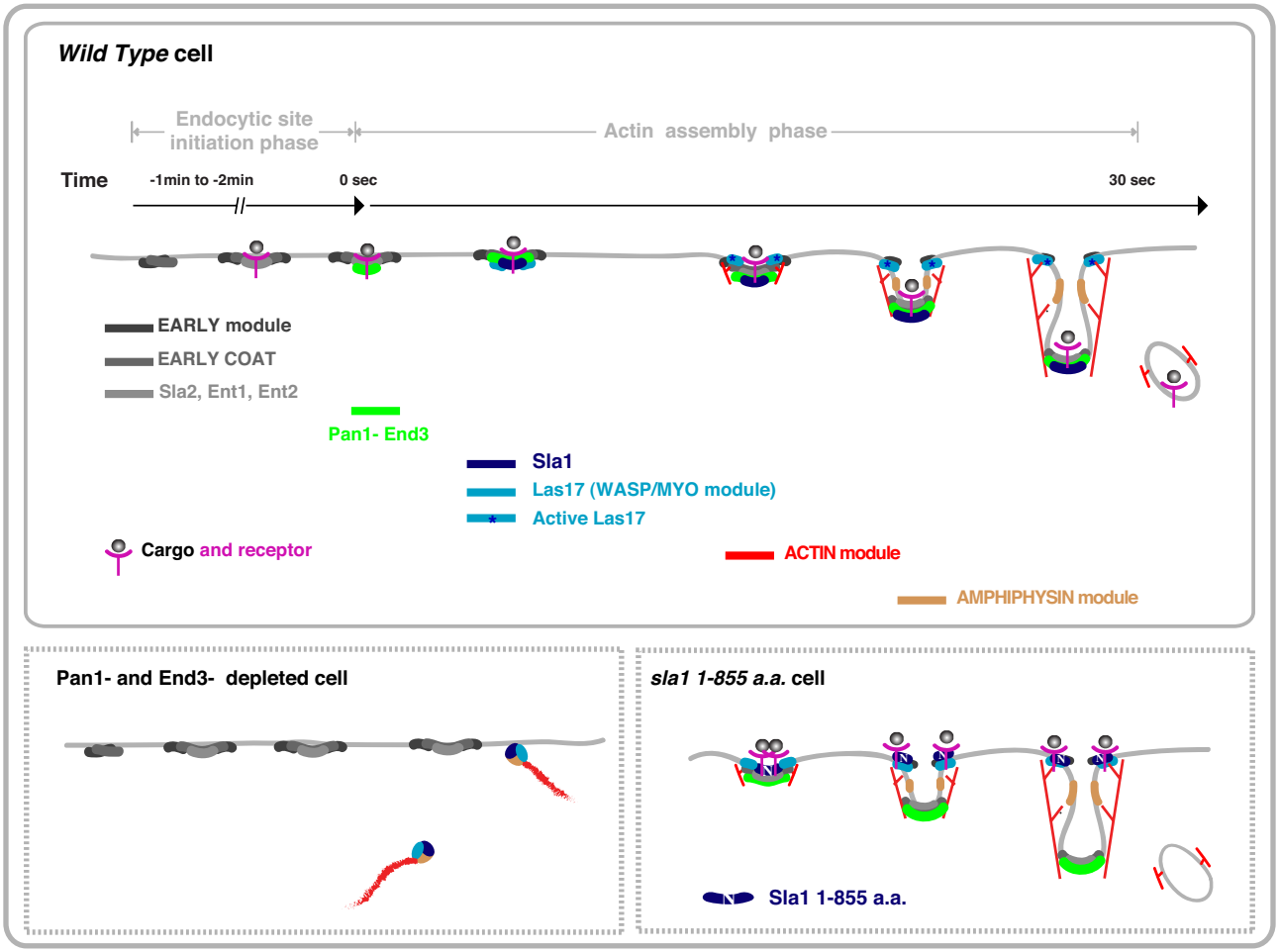

FIGURE 9: Molecular basis for coordination of receptors, adaptors, and the actin machinery at endocytic sites. See the text for a detailed description.

Sla1 N-terminal region might be masked and therefore unable to access endocytic sites or the nucleus.

The Pan1-End3 complex coordinates cargo capture with endocytic actin assembly

In the absence of Pan1 and End3, the endocytic-site initiation and actin machinery assembly phases are spatially uncoupled (Figures 5 and 6). Many proteins appearing during endocytic-site initiation function in cargo recruitment. Here our observations provide new mechanistic insights into how Pan and End3 coordinate cargo capture with endocytic actin assembly through their interactions with Sla1. However, without Sla1, the actin assembly machinery can still be recruited to and function at endocytic sites, although with reduced efficiency (Kaksonen *et al.*, 2005). Sla1 is known to mediate NPFXD-mediated endocytosis but not other types of endocytosis, such as ubiquitin-directed endocytosis (Howard *et al.*, 2002). Thus Sla1 is likely not the only "downstream linker" through which Pan1-End3 couples cargoes to the actin assembly machinery.

Pan1 contains a WH2-acidic (WA) domain at its C-terminus and may therefore assist in actin nucleation when Las17 recruitment is defective in the absence of Sla1 (Sun *et al.*, 2006). In addition, Pan1 was reported to interact with type I myosin (Barker *et al.*, 2007), which is another key mediator of actin assembly and force production (Sirotkin *et al.*, 2005; Sun *et al.*, 2006). Further, the N-terminal EH domains of Pan1 and End3 were previously shown to bind to Ent1/2 (yeast epsin) and Yap1801/2 (yeast AP180/CALM; Wendland and Emr, 1998), all of which may also function as endocytic adaptors (Reider and Wendland, 2011). Thus Pan1-End3 likely plays a general role coordinating cargo accumulation with actin assembly through multiple binding partners in addition to Sla1, thereby maintaining endocytic internalization as a robust process and ensuring that cargo capture occurs before endocytic vesicle formation mediated by the endocytic actin machinery.

Of importance, proteins homologous to Pan1, End3, and Sla1 are present in mammalian cells (Dupre *et al.*, 2004). Eps15 (mammalian homologue of Pan1 and End3) and CIN85 (mammalian homologue of Sla1) both play important, yet poorly defined roles in endocytosis. Our results suggest possible Eps15 and CIN85 functions.

MATERIALS AND METHODS

Media, strains, and plasmids

Yeast strains were grown in standard rich medium (yeast extract/peptone/dextrose [YPD]) or synthetic medium (SD) supplemented with the appropriate amino acids. The yeast strains are listed in Supplemental Table S1. GFP, mCherry, RFP, and AID tags were integrated at the C-terminus of each gene as described previously (Longtine *et al.*, 1998; Nishimura *et al.*, 2009; Morawska and Ulrich, 2013; Eng *et al.*, 2014).

Fluorescence microscopy and image analysis

Fluorescence microscopy was performed using a Nikon Eclipse Ti microscope (Nikon Instruments, Melville, NY) controlled by MetaMorph (Molecular Devices, Sunnyvale, CA), equipped with a Plan Apo VC 100×/1.4 Oil OFN25 DIC N2 objective (with Type NF immersion oil; Nikon), a Perfect Focus System (Nikon), and a Neo sCMOS camera (Andor Technology, South Windsor, CT; 65-nm effective pixel size). For live-cell imaging, cells were grown to early log phase at 25°C. The cells in synthetic media were adhered to the surface of a concanavalin A–coated (0.1 µg/ml) coverslip. All imaging was done at room temperature. For single-channel live-cell imaging, images were acquired continuously at 1–2 frames/s, depending on the signal intensity. Two-channel movies were made using the SPECTRA X Light Engine (Lumencor, Beaverton, OR) for excitation with a 524/628-nm dual-band bandpass filter for GFP/mCherry emission (Brightline; Semrock, Lake Forest, IL).

To compare the appearance timing of GFP- and mCherry-tagged proteins, data from the GFP or mCherry channel of a two-color movie were analyzed by open-source image analysis software Icy (de Chaumont *et al.*, 2012). The software automatically detected the fluorescent spots that are significantly brighter than the cell background with a wavelet-based detection algorithm implemented as a plug-in (Spot Detector plug-in). The results were visually confirmed by comparing trajectories to the original movie. Patches that at any point in their lifetime were too close to another patch to be clearly resolved were excluded from our analysis. The development of fluorescence intensity of GFP- or mCherry-tagged proteins was quantified using ImageJ software (National Institutes of Health, Bethesda, MD). For this analysis, intensities were corrected for photobleaching (Kaksonen *et al.*, 2003).

Montages and kymographs were generated from indicated movies using ImageJ software. To quantitatively compare cortical localization of endocytic proteins in different strains or under different conditions, the total number of endocytic patches was counted for each cell during the duration of the indicated movie. The total patch number was then divided by the cell perimeter (micrometers). Twenty cells were analyzed for each strain or condition. The average and SD for the patch number per micrometer were calculated. The percentage change in patch cortical localization between strains or conditions was calculated by dividing the average patch number per cell perimeter for one strain or condition by the other.

Yeast extract preparation and gel filtration chromatography

Yeast were grown to an OD_{600} of ~1.2 at 30°C in YPD before pelleting and washing in 4°C double-distilled H_2O. The pellets were flash-frozen in liquid N_2 and pulverized using a 6870 Freezer/Mill (SPEX SamplePrep, Metuchen, NJ). The efficiency of cell disruption was monitored microscopically and judged to be >90%. To each gram of yeast powder, 1 ml of buffer (100 mM (4-(2-hydroxyethyl)-1-piperazineethanesulfonic acid [HEPES], 300 mM NaCl, 2 mM ethylene glycol tetraacetic acid [EGTA], 2 mM dithiothreitol, pH 7.4) and protease inhibitors (Protease Inhibitor Cocktail Set IV; Calbiochem, Merck4Biosciences, Billerica, CA) were added. Yeast powder was gently mixed on ice with the buffer and centrifuged for 20 min at 350,000 × *g*. The cleared supernatant (~20 mg/ml) was collected for gel filtration chromatography. Gel filtration was carried out with a Superose 6 column (Amersham Biosciences, Piscataway, NJ) connected to a fast protein liquid chromatography system (Amersham Biosciences) and equilibrated with buffer (50 mM HEPES, 150 mM NaCl, 1 mM EGTA, 1 mM dithiothreitol, pH 7.4). Elution was performed at a flow rate of 0.4 ml/min at 4°C. Fractions (0.75 ml) were collected and analyzed by immunoblotting or immunoprecipitation-immunoblotting.

ACKNOWLEDGMENTS

We thank the members of the Drubin lab for helpful discussions. We are grateful to Itziar Ibarlucea, Anthony Cormier, and Sun Hae Hong for advice on gel filtration chromatography and image analysis. We also thank Ross Pedersen, Christa Cortesio, Charlotte Kaplan, Emily Stoops, Itziar Ibarlucea, Rebecca Lu, and Nathaniel Krefman for critical reading of the manuscript. This work was supported by National Institutes of Health Grants R01 GM50399 and R01 GM42759 to D.G.D.

REFERENCES

Barker SL, Lee L, Pierce BD, Maldonado-Baez L, Drubin DG, Wendland B (2007). Interaction of the endocytic scaffold protein Pan1 with the type I myosins contributes to the late stages of endocytosis. Mol Biol Cell 18, 2893–2903.

Benedetti H, Raths S, Crausaz F, Riezman H (1994). The END3 gene encodes a protein that is required for the internalization step of endocytosis and for actin cytoskeleton organization in yeast. Mol Biol Cell 5, 1023–1037.

Boeke D, Trautmann S, Meurer M, Wachsmuth M, Godlee C, Knop M, Kaksonen M (2014). Quantification of cytosolic interactions identifies Ede1 oligomers as key organizers of endocytosis. Mol Syst Biol 10, 756.

Boettner DR, Chi RJ, Lemmon SK (2012). Lessons from yeast for clathrin-mediated endocytosis. Nat Cell Biol 14, 2–10.

Brach T, Godlee C, Moeller-Hansen I, Boeke D, Kaksonen M (2014). The initiation of clathrin-mediated endocytosis is mechanistically highly flexible. Curr Biol 24, 548–554.

Bradford MK, Whitworth K, Wendland B (2015). Pan1 regulates transitions between stages of clathrin-mediated endocytosis. Mol Biol Cell 26, 1372–1385.

Carroll SY, Stimpson HE, Weinberg J, Toret CP, Sun Y, Drubin DG (2012). Analysis of yeast endocytic site formation and maturation through a regulatory transition point. Mol Biol Cell 23, 657–668.

Chi RJ, Torres OT, Segarra VA, Lansley T, Chang JS, Newpher TM, Lemmon SK (2012). Role of Scd5, a protein phosphatase-1 targeting protein, in phosphoregulation of Sla1 during endocytosis. J Cell Sci 125, 4728–4739.

Confalonieri S, Di Fiore PP (2002). The Eps15 homology (EH) domain. FEBS Lett 513, 24–29.

de Chaumont F, Dallongeville S, Chenouard N, Herve N, Pop S, Provoost T, Meas-Yedid V, Pankajakshan P, Lecomte T, Le Montagner Y, *et al.* (2012). Icy: an open bioimage informatics platform for extended reproducible research. Nat Methods 9, 690–696.

Doherty GJ, McMahon HT (2009). Mechanisms of endocytosis. Annu Rev Biochem 78, 857–902.

Duncan MC, Cope MJ, Goode BL, Wendland B, Drubin DG (2001). Yeast Eps15-like endocytic protein, Pan1p, activates the Arp2/3 complex. Nat Cell Biol 3, 687–690.

Dupre S, Urban-Grimal D, Haguenauer-Tsapis R (2004). Ubiquitin and endocytic internalization in yeast and animal cells. Biochim Biophys Acta 1695, 89–111.

Eng T, Guacci V, Koshland D (2014). ROCC, a conserved region in cohesin's Mcd1 subunit, is essential for the proper regulation of the maintenance of cohesion and establishment of condensation. Mol Biol Cell 25, 2351–2364.

Feliciano D, Di Pietro SM (2012). SLAC, a complex between Sla1 and Las17, regulates actin polymerization during clathrin-mediated endocytosis. Mol Biol Cell 23, 4256–4272.

Gardiner FC, Costa R, Ayscough KR (2007). Nucleocytoplasmic trafficking is required for functioning of the adaptor protein Sla1p in endocytosis. Traffic 8, 347–358.

Goley ED, Welch MD (2006). The ARP2/3 complex: an actin nucleator comes of age. Nat Rev Mol Cell Biol 7, 713–726.

Howard JP, Hutton JL, Olson JM, Payne GS (2002). Sla1p serves as the targeting signal recognition factor for NPFX(1,2)D-mediated endocytosis. J Cell Biol 157, 315–326.

Kaksonen M, Sun Y, Drubin DG (2003). A pathway for association of receptors, adaptors, and actin during endocytic internalization. Cell 115, 475–487.

Kaksonen M, Toret CP, Drubin DG (2005). A modular design for the clathrin- and actin-mediated endocytosis machinery. Cell 123, 305–320.

Longtine MS, McKenzie A 3rd, Demarini DJ, Shah NG, Wach A, Brachat A, Philippsen P, Pringle JR (1998). Additional modules for versatile and economical PCR-based gene deletion and modification in Saccharomyces cerevisiae. Yeast 14, 953–961.
McMahon HT, Boucrot E (2011). Molecular mechanism and physiological functions of clathrin-mediated endocytosis. Nat Rev Mol Cell Biol 12, 517–533.
Merrifield CJ, Feldman ME, Wan L, Almers W (2002). Imaging actin and dynamin recruitment during invagination of single clathrin-coated pits. Nat Cell Biol 4, 691–698.
Michelot A, Costanzo M, Sarkeshik A, Boone C, Yates JR 3rd, Drubin DG (2010). Reconstitution and protein composition analysis of endocytic actin patches. Curr Biol 20, 1890–1899.
Mooren OL, Galletta BJ, Cooper JA (2012). Roles for actin assembly in endocytosis. Annu Rev Biochem 81, 661–686.
Morawska M, Ulrich HD (2013). An expanded tool kit for the auxin-inducible degron system in budding yeast. Yeast 30, 341–351.
Nishimura K, Fukagawa T, Takisawa H, Kakimoto T, Kanemaki M (2009). An auxin-based degron system for the rapid depletion of proteins in nonplant cells. Nat Methods 6, 917–922.
Reider A, Wendland B (2011). Endocytic adaptors—social networking at the plasma membrane. J Cell Sci 124, 1613–1622.
Rodal AA, Manning AL, Goode BL, Drubin DG (2003). Negative regulation of yeast WASp by two SH3 domain-containing proteins. Curr Biol 13, 1000–1008.
Sachs AB, Deardorff JA (1992). Translation initiation requires the PAB-dependent poly(A) ribonuclease in yeast. Cell 70, 961–973.
Sirotkin V, Beltzner CC, Marchand JB, Pollard TD (2005). Interactions of WASp, myosin-I, and verprolin with Arp2/3 complex during actin patch assembly in fission yeast. J Cell Biol 170, 637–648.
Skruzny M, Brach T, Ciuffa R, Rybina S, Wachsmuth M, Kaksonen M (2012). Molecular basis for coupling the plasma membrane to the actin cytoskeleton during clathrin-mediated endocytosis. Proc Natl Acad Sci USA 109, E2533–E2542.
Sun Y, Kaksonen M, Madden DT, Schekman R, Drubin DG (2005). Interaction of Sla2p's ANTH domain with PtdIns(4,5)P2 is important for actin-dependent endocytic internalization. Mol Biol Cell 16, 717–730.
Sun Y, Martin AC, Drubin DG (2006). Endocytic internalization in budding yeast requires coordinated actin nucleation and myosin motor activity. Dev Cell 11, 33–46.
Suzuki R, Toshima JY, Toshima J (2012). Regulation of clathrin coat assembly by Eps15 homology domain-mediated interactions during endocytosis. Mol Biol Cell 23, 687–700.
Tang HY, Munn A, Cai M (1997). EH domain proteins Pan1p and End3p are components of a complex that plays a dual role in organization of the cortical actin cytoskeleton and endocytosis in Saccharomyces cerevisiae. Mol Cell Biol 17, 4294–4304.
Tang HY, Xu J, Cai M (2000). Pan1p, End3p, and S1a1p, three yeast proteins required for normal cortical actin cytoskeleton organization, associate with each other and play essential roles in cell wall morphogenesis. Mol Cell Biol 20, 12–25.
Toshima J, Toshima JY, Duncan MC, Cope MJ, Sun Y, Martin AC, Anderson S, Yates JR 3rd, Mizuno K, Drubin DG (2007). Negative regulation of yeast Eps15-like Arp2/3 complex activator, Pan1p, by the Hip1R-related protein, Sla2p, during endocytosis. Mol Biol Cell 18, 658–668.
Weinberg J, Drubin DG (2012). Clathrin-mediated endocytosis in budding yeast. Trends Cell Biol 22, 1–13.
Welch MD, Way M (2013). Arp2/3-mediated actin-based motility: a tail of pathogen abuse. Cell Host Microbe 14, 242–255.
Wendland B, Emr SD (1998). Pan1p, yeast eps15, functions as a multivalent adaptor that coordinates protein-protein interactions essential for endocytosis. J Cell Biol 141, 71–84.
Wendland B, McCaffery JM, Xiao Q, Emr SD (1996). A novel fluorescence-activated cell sorter-based screen for yeast endocytosis mutants identifies a yeast homologue of mammalian eps15. J Cell Biol 135, 1485–1500.
Whitworth K, Bradford MK, Camara N, Wendland B (2014). Targeted disruption of an EH-domain protein endocytic complex, Pan1-End3. Traffic 15, 43–59.